

# DESIGN OF A PHYSICAL MODEL OF THE PBMR WITH THE AID OF FLOWNET

G.P. GREYVENSTEIN and P.G. ROUSSEAU

*Department of Mechanical Engineering*

*Potchefstroom University for Christian Higher Education, Potchefstroom, 2531, South Africa*

## ABSTRACT

The design of a physical model of the PBMR with the aid of the code Flownet is discussed in this paper. The purpose of the physical model is to test the control strategies and operating procedures of the PBMR and also to demonstrate the accuracy of Flownet. Flownet is first used to do component matching and to determine the detail steady-state performance of the system. It is then demonstrated how the code was used to simulate the start-up procedure as well as a load following and a load rejection scenario. The study demonstrates how a micro model of the PBMR can be designed with the aid of a powerful simulation tool in a relatively short period of time and at low cost using commercially available turbochargers.

## 1. Introduction

The Pebble Bed Modular Reactor (PBMR) is a new type of high temperature gas nuclear power plant that is currently being developed by the South African utility ESKOM. The PBMR is based on closed cycle three-shaft recuperative Brayton cycle and it uses helium as the working fluid.

Although it is relatively easy to predict the steady-state performance of a plant such as the PBMR the prediction of the dynamic behaviour of the PBMR, which is required for the design of the control system, presents unique challenges. A great effort was therefore put into the development of a powerful new dynamic modelling tool, called Flownet.

One of the distinguishing features of the PBMR, which complicates the design of the control system, is the use of three separate shafts for the different compressor/turbine and turbine/generator pairs as opposed to one or two shafts used in other designs. In order to test the control strategies of the PBMR and also to demonstrate the accuracy of Flownet, it was decided to develop a micro model of the power conversion cycle of the PBMR. The model will use an electrical heater to emulate the nuclear reactor. Since the objective of the micro model is not to address specific issues related to the use of helium as the working fluid or to test the performance of individual components such as compressors, turbines or heat exchangers, it was decided to use nitrogen instead of helium as the working fluid. This makes it possible to use off-the-shelf single stage centrifugal compressors and turbines instead of more expensive multi-stage centrifugal or axial flow machines. It should be stressed that the micro model is not a scale model of the prototype plant but a system that will have the same characteristics and degrees of freedom and therefore also the same control topology as the prototype plant.

In this paper the design of the micro model with the aid of Flownet will be discussed. Emphasis will be placed on modelling of transient phenomena such as start-up, power control and load rejection.

## 2. The PBMR power conversion cycle and comparison with the micro model

A schematic layout of the PBMR power conversion cycle is shown in Figure 1. Starting at 1, helium at a relatively low pressure and temperature is compressed by a low-pressure compressor (LPC) to an intermediate pressure (2) after which it is cooled in an intercooler to state 3. A high-pressure compressor (HPC) then compresses the helium to state 4. From 5 to 6 the helium is preheated in the recuperator before entering the reactor, which heats the helium to state 8. After the reactor the hot high-pressure helium is expanded in a high-pressure turbine (HPT) to state 9 after which it is further expanded in a low-pressure turbine (LPT) to state 11. The high-pressure turbine drives the high-pressure compressor while the low-pressure turbine is drives the low-pressure compressor. After the

low pressure turbine the helium is further expanded in the power turbine to pressure 13. From 13 to 14 the still hot helium is cooled in the recuperator after which it is further cooled in the pre-cooler to state 1. This completes the cycle. The heat rejected from 13 to 14 is equal to the heat transferred to the helium from 5 to 6.

The output of the plant can be controlled by changing the helium inventory of the system or by opening and closing of the bypass valve (BPV). Changing of the helium inventory is a relatively slow process and is used for load following while the faster bypass control is used for load rejection.

Although the design of the micro model closely resembles that of the PBMR plant it is important to highlight the following differences:

- (i) The micro model will use nitrogen instead of helium as the working fluid. This will not subtract from the objective of the model which is not to address specific issues related to the use of helium as the working fluid but to develop a system that will have the same overall characteristics as that of the prototype plant.
- (ii) The micro model will use cheap off-the-shelf single stage centrifugal compressors and turbines rather than axial flow machines. The performance characteristics of centrifugal machines closely resembles that of axial flow machines and it will therefore suffice for the purpose of this project.
- (iii) In the micro model the nuclear reactor will be emulated by an electrical resistance heater, which will, like the pebble bed reactor, have a large thermal capacity.
- (iv) The generator will be emulated by a load compressor connected to a power dissipation loop consisting of a flow control valve and a heat exchanger as shown in Figure 2. Variations in load can be affected by increasing or decreasing the pressure level in the load rejection loop.

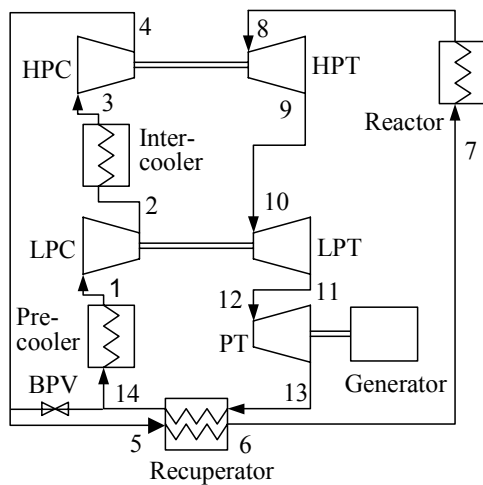


Fig 1. Schematic layout of the PBMR recuperative Brayton cycle.

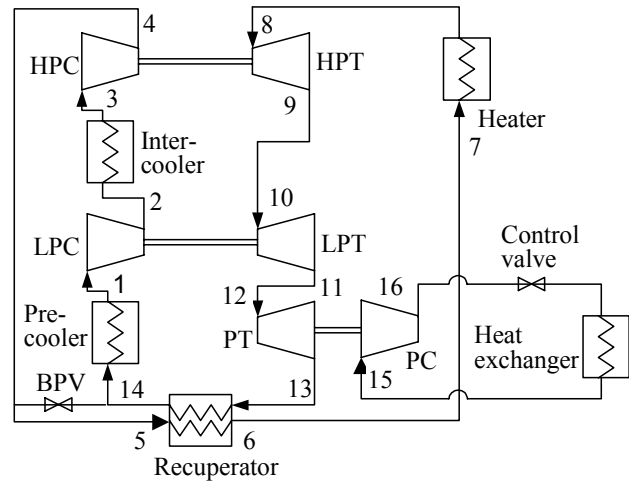


Fig 2. Layout of the micro model cycle.

### 3. First-order cycle analysis

The first step in the design of the micro model was to do a first-order cycle analysis to determine a suitable operating point for the system. Figures 3 and 4 show the result of this analysis with the following assumptions: compressor efficiency = 75 percent, turbine efficiency = 72 percent, pre-cooler and inter-cooler outlet temperature = 26 °C, heater outlet temperature 700 °C, turbocharger mechanical efficiency = 98 percent, pipe pressure loss = 2 percent of inlet absolute pressure and heat exchanger pressure loss = 10 percent of inlet absolute pressure.

As can be seen from Figure 3 the cycle efficiency increases with recuperator efficiency over the whole range of pressure ratios. At a recuperator efficiency of 1.0 the cycle efficiency decreases with pressure ratio while it shows an optimum at recuperator efficiencies of smaller than 0.95. Figure 4 shows that the specific work increases with pressure ratio irrespective of the recuperator efficiency.

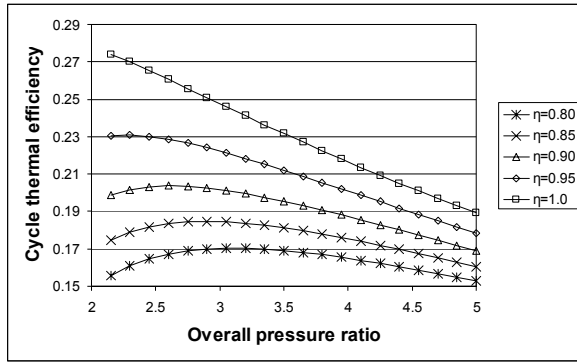


Fig 3. Thermal efficiency as function of recuperator efficiency and overall pressure ratio.

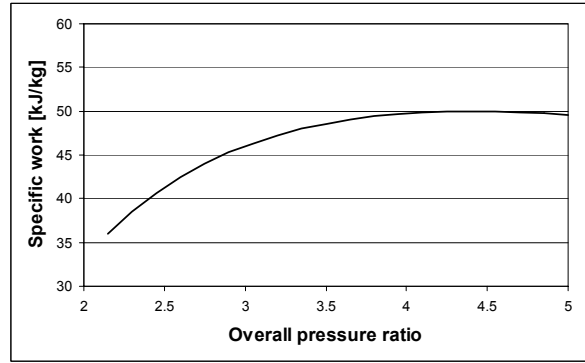


Fig 4. Specific work as function of overall pressure ratio.

The recuperator efficiency is a function of the product of the area and the overall heat transfer coefficient of the recuperator and is therefore a design choice. Since the area and therefore also the price of the recuperator increases exponentially with area, an efficiency of approximately 0.85 was chosen as a good compromise between performance and cost. Figure 3 shows that at a recuperator efficiency of 0.85 the cycle efficiency is a maximum at a pressure ratio of approximately 2.75. Figure 4 on the other hand shows that the specific work is a maximum at a pressure ratio of approximately 4.5. Since both cycle efficiency and specific work are important and since cycle efficiency is not as sensitive to pressure ratio as specific work, it was decided to design for an overall pressure ratio of approximately 4, which is a good compromise between efficiency and specific work.

#### 4. Selection of turbochargers

The operating points of the turbo machines are determined by the system operating point and are expressed in terms of pressure ratio and non-dimensional mass flow, which is defined as

$$\bar{m} = \frac{\dot{m}\sqrt{T_0}}{p_0} \quad (1)$$

where  $\dot{m}$  = mass flow rate,  $T_0$  = total inlet temperature and  $p_0$  = total inlet pressure. Table 1 shows the pressure ratio and non-dimensional mass flow for a mass flow of 1 kg/s and a system pressure of 100 kPa at the inlet of the low-pressure compressor.

Turbo unit	Pressure ratio	Non-dimensional mass flow [kg/s $\sqrt{K/bar}$ ]
Low pressure compressor	2.0	17.3
High pressure compressor	2.0	8.7
High pressure turbine	1.6	8.1
Low pressure turbine	1.7	12.4
Power turbine	1.4	20.0

Table 1. Operating points of the different turbo machines for a mass flow of 1 kg/s and LP compressor inlet pressure of 100 kPa.

As can be seen from Table 1, the power turbine, although having the lowest pressure ratio, has the largest non-dimensional mass flow. The procedure that was therefore followed was to select the turbocharger with the largest turbine from a range of commercially available units. The turbine of this unit has a non-dimensional mass flow of 10.8 at a pressure ratio of 1.4. This fixes the cycle mass flow at a value of  $10.8/20 = 0.54$  kg/s at a pressure level of 100 kPa at the inlet to the LP compressor.

Table 2 shows the recalculated non-dimensional mass flows along with the power rating of the different turbo machines for a cycle mass flow of 0.54 kg/s. The scaling of mass flows does not affect the pressure ratios.

Turbo unit	Pressure ratio	Non-dimensional mass flow [kg/s $\sqrt{K/bar}$ ]	Power [kW]
Low pressure compressor	2.0	9.3	47.4
High pressure compressor	2.0	4.7	47.4
High pressure turbine	1.6	4.4	48.4
Low pressure turbine	1.7	6.7	48.4
Power turbine	1.4	10.8	27.4

Table 2. Pressure ratio, non-dimensional mass flow and power for a mass flow of 0.54 kg/s and LP compressor inlet pressure of 100 kPa.

With the pressure ratio and non-dimensional mass flows of the other turbines known from Table 2, turbochargers were selected whose turbines match these operating points the closest. The suitability of the compressors was verified with the aid of Flownet, which solves for the speed of the different turbochargers.

## 5. Modelling of the system with Flownet

Flownet is a general thermal-fluid network analysis code that can model both steady-state and transient flows. Its solver, described elsewhere [1], is based on an Implicit Pressure Correction Method (IPCM) and solves for the conservation of mass and energy at all nodes and momentum in all elements. The code can deal with a wide range of standard network components such as compressors, turbines, pipes, diffusers, valves, heat exchangers and pebble bed nuclear reactors. Flownet can also deal with heat transfer between flow elements and solid structures as well as heat transfer through the solid structures. Important to mention is that heat exchangers are not handled as lumped systems but as distributed systems [2]. This is necessary to more accurately deal with the thermal capacitance of the metal separating the hot and cold streams. Flownet has been extensively validated against experimental results, other codes and analytical solutions.

Input data of compressors and turbines are provided in the form of performance maps, which gives the pressure ratio as function of non-dimensional speed,  $N/\sqrt{T_0}$ , and non-dimensional mass flow,  $\dot{m} \sqrt{T_0/p_0}$ , for different geometries such as blade angle. Any number of compressor or turbine stages as well as external loads can be placed on a single shaft and steady-state load balancing can be done by varying either the shaft speed or the master turbine geometry, typically the blade angle. In the case of transient flows Flownet calculates the shaft speed transients by taking the inertia of all rotating parts into account.

Modelling of the cycle by Flownet requires compilation of detail input data for all components such as pipes, diffusers, valves, volumes and heat exchangers. Although space does not allow us to discuss the design of the system in detail the diameters of interconnection piping and the design of heat exchangers will be given.

Pipes that connect the major components have a diameter of 200 mm, except the pipe between the power turbine outlet and the recuperator, which has a diameter of 250 mm. All heat exchangers, including the recuperator, are of a shell-and tube design with one shell pass and one tube pass. In the case of the pre-cooler, intercooler and load rejection heat exchanger the gas flows through the tube side with water flowing through the shell side, while in the case of the recuperator the low pressure hot gas coming from the LP turbine flows through the tube side with the high pressure gas from the HP compressor flowing through the shell side.

The details of the different heat exchangers are given in Table 3.

Heat exchanger	Length between tube sheets [m]	Tube inside diameter [mm]	Number of tubes	Heat transfer area[m <sup>2</sup> ]	Tube mass [kg]
Pre-cooler	2.1	10.22	575	48	513
Intercooler	1.9	10.22	450	35	363
Load rejection	2.4	10.22	450	43	460
Recuperator	5.8	10.22	1075	255	2728

Table 3. Design of the different heat exchangers.

The Flownet steady-state results for two different pressure levels are given in Table 4.

Component	LP compressor inlet pressure = 100 kPa						LP compressor inlet pressure = 250 kPa					
	P <sub>in</sub> [kPa]	P <sub>out</sub> [kPa]	T <sub>in</sub> [°C]	T <sub>out</sub> [°C]	Rating [kW]	Speed [rpm]	P <sub>in</sub> [kPa]	P <sub>out</sub> [kPa]	T <sub>in</sub> [°C]	T <sub>out</sub> [°C]	Rating [kW]	Speed [rpm]
LP Compressor	100.0	200.8	22.9	109.6	51.0	72078	250.0	496.9	26.0	112.1	124.3	71811
LP Turbine	248.5	150.5	628.5	549.0	51.0	72078	611.7	372.1	628.8	549.8	124.3	71811
HP Compressor	198.4	381.9	22.9	102.3	46.7	70009	491.3	938.0	26.1	105.1	114.1	69842
HP Turbine	378.0	249.1	700.0	628.5	46.7	70009	929.2	613.2	700.0	628.8	114.1	69842
Power Compressor	105.0	150.7	21.1	65.9	32.1	39073	262.0	372.1	22.9	66.6	76.8	38707
Power Turbine	149.7	105.0	549.0	498.2	32.1	39073	370.2	262.0	549.8	500.4	76.8	38707
Precooler	101.1	100.5	165.3	22.9	83.9	-	252.4	251.2	155.1	26.0	186.6	-
Intercooler	199.1	198.7	109.6	22.9	50.9	-	492.8	491.9	112.1	26.1	124.1	-
Recuperator hot side	103.0	102.3	498.2	165.3	202.6	-	257.1	255.2	500.4	155.1	515.6	-
Recuperator cold side	381.1	379.4	102.3	438.8	202.6	-	935.9	932.5	105.1	453.3	515.6	-
Load rejection HX	106.5	105.1	65.9	21.1	32.1	-	265.1	262.3	66.6	22.9	76.8	-

Table 4. Steady-state results for two pressure levels i.e. 100 kPa and 250 kPa at the inlet to the LP compressor.

Interesting to note is that the recuperator efficiency is 84 percent in the case of the lower pressure level and 87 percent in the case of the higher pressure level. This is due to the fact that the flow in the recuperator is laminar at the lower pressure level and turbulent at the higher pressure level.

## 6. Simulation of start-up

The system is started by forcing nitrogen through it by an inline blower placed just before the LP compressor while at the same time adding heat in the heater. The simulation starts with the steady-state solution at a point where the heater exit temperature is 400 °C and the LP compressor inlet pressure is 100 kPa. The heat input is now increased at such a rate that the heater exit temperature increases 50 °C/s until the exit temperature reaches a value of 700 °C where after it is kept constant at this value. During this process the pressure rise across the blower decreases. At the point where the pressure rise becomes zero the by-pass valve across the blower is opened and the blower is isolated from the main loop. From here onwards the system runs on its own.

Figure 5 shows the variation in turbine speeds and Figure 6 the variation in pressures during start-up. The speed of all the turbo chargers increases as expected and steady-state is reached in approximately 100 s. The pressure at the HP compressor outlet increases while the pressure at the inlet to the LP compressor decreases. This behaviour is due to the fact that the inventory is kept constant during the start-up.

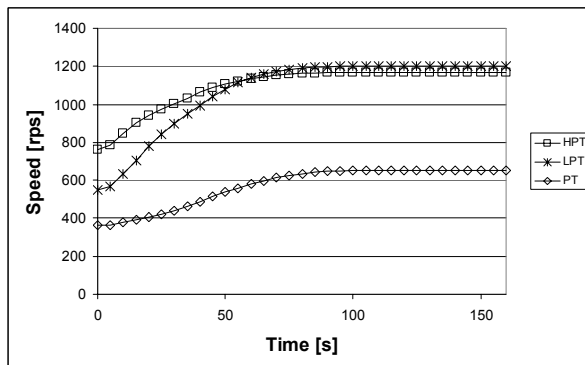


Fig 5. Variation in turbine speed during start-up.

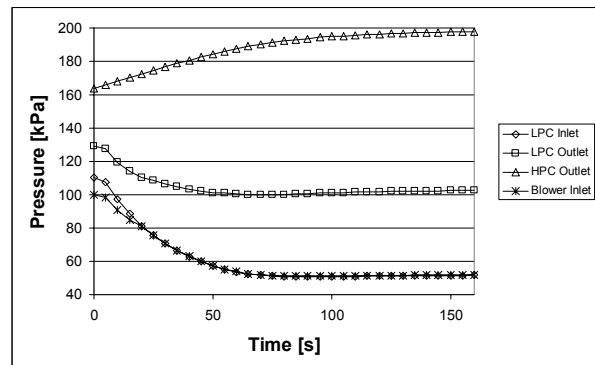


Fig 6. Variation in pressure during start-up

The time step for this simulation was 0.5 s and execution time was approximately 0.2 s per time step on a 700 MHz Pentium III processor.

## 7. Power control

The power output of the system can be controlled by increasing or decreasing the mass inventory in the system. The issue that needs to be resolved is exactly where to inject or extract the mass. The two most obvious possibilities are either before the LP compressor (position 1, Fig. 2) or after the HP compressor (position 4, Fig 2).

Figure 7 shows the variation in power for the case where the mass is injected and extracted before the LP compressor. The simulation starts at steady-state conditions at a power level of 100 kPa (at position 1) and a heater outlet temperature of 700 °C. At time  $t = 1$  s mass is injected into the system at a rate of 0.1 kg/s for 400 s where after the system is allowed to stabilise for 100 s. Thereafter mass is extracted at a rate of 0.1 kg/s for another 400 s after which the system is again allowed to stabilise. Fig. 8 shows the variation in speed of the three turbochargers during the transient.

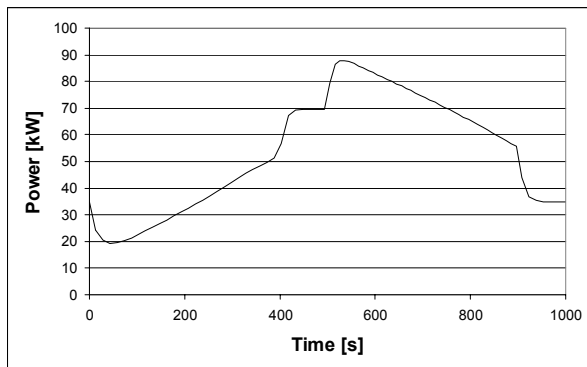


Fig 7. Variation in power when mass is injected and extracted before the LP compressor.

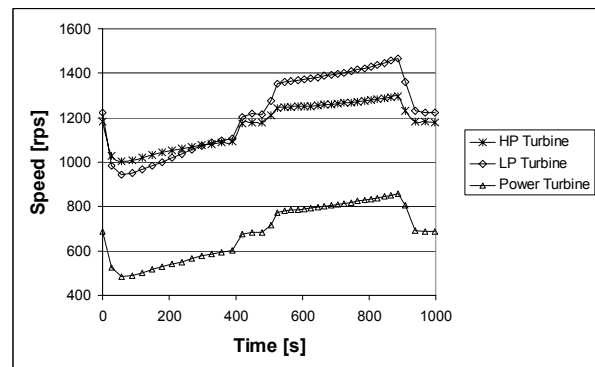


Fig 8. Variation in turbocharger speed when mass is injected and extracted before the LP compressor.

Figure 7 shows that the power first decreases before it starts to increase when mass is injected into the system and visa versa. This behaviour, which is undesirable, is due to the immediate increase in the back pressure of the power turbine when one starts to inject mass before the LP compressor. If mass is injected too fast the system can shut-down.

Figure 9 shows the variation in power for the case where the mass is injected and extracted after the HP compressor. The simulation starts at steady-state conditions at a power level of 100 kPa (at position 1) and a heater outlet temperature of 700 °C. At time  $t = 1$  s mass is injected into the system at a rate of 1 kg/s for 37 s where after the system is allowed to stabilise for 42 s. Thereafter mass is extracted at a rate of 1 kg/s for another 37 s after which the system is again allowed to stabilise. Fig. 10 shows the variation in speed of the three turbochargers during the transient.

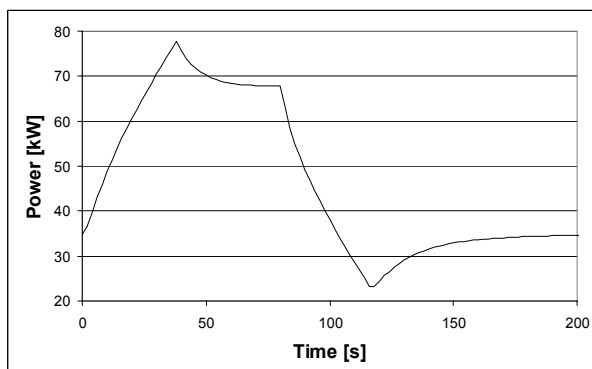


Fig 9. Variation in power when mass is injected and extracted after the HP compressor.

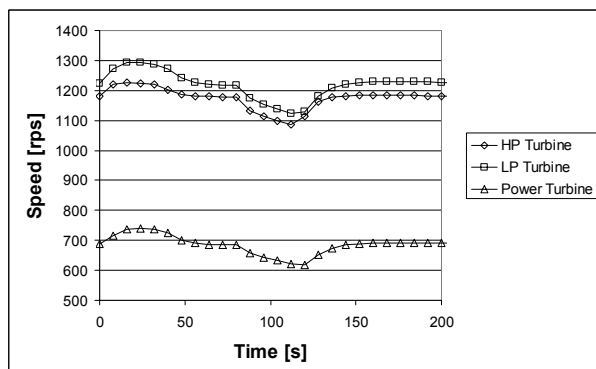


Fig 10. Variation in turbocharger speed when mass is injected and extracted after the HP compressor.

Figure 9 shows that the power output immediately starts to increase when mass is injected after the HP compressor and immediately starts to decrease when mass is extracted. Mass can therefore be injected and extracted at a much faster rate to follow rapid changes in load. Comparing Figures 8 and 10 one

can also conclude that the turbocharger speeds do not fluctuate as much in the case of mass injection and extraction at position 4 as compared to injection and extraction at position 1.

Simulations in this section were done for a time step of 0.2 s and execution time was approximately 0.2 s per time step.

## 8. Load rejection

Load rejection is done by suddenly opening the bypass valve between the high pressure and low pressure sides, shown in Figure 2. Figures 11 and 12 show the variation in power and speeds of the turbochargers respectively during a load rejection scenario. The initial condition for this scenario is the steady-state solution for a pressure level of 250 kPa (at position 1 in Figure 2) and a heater outlet temperature of 700 °C.

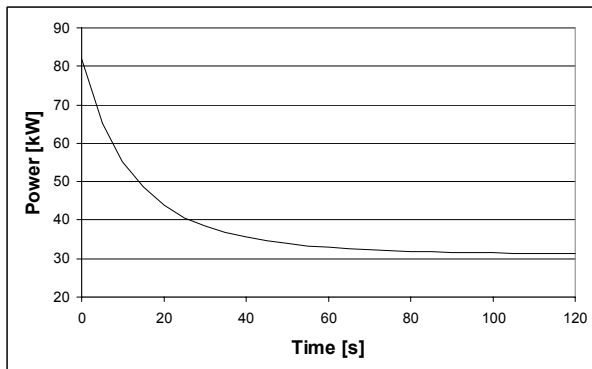


Fig 9. Variation in power during a load rejection.

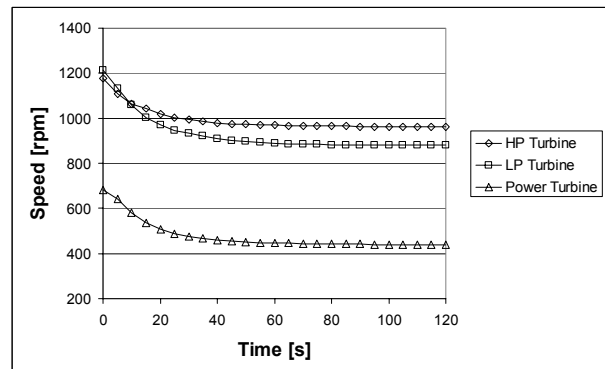


Fig 10. Variation in turbocharger speed during a load rejection.

Figure 9 shows that the power drops from 80 kW to 31 kW (or 61 percent) in approximately 90 s. The valve opening for this case was 15 mm. If the valve opening is increased the system shuts down. Figure 10 shows that the turbocharger speeds also drop significantly during the transient.

## 9. Conclusion

The design of a physical model of the PBMR with the aid of the thermal-fluid network simulation code Flownet was discussed in this paper. The study showed that it is not only feasible to build a physical model of the PBMR using off the shelf turbochargers, but that all the major operating procedures such as start-up, power variation and load rejection can be demonstrated on the micro model. The study also demonstrated the utility of a powerful simulation tool such as Flownet in the design of the micro model.

## 10. Acknowledgement

This study was sponsored by PBMR (Pty.) Ltd., a subsidiary of the South African utility ESKOM, and the National Research Foundation. The authors want to thank Mr. Walter Crommelin, a visiting student from TU Delft, for his valuable assistance.

## 11. References

- [1] G.P. Greyvenstein, An implicit method for the analysis of transient flows in pipe networks, *International Journal for Numerical Methods in Engineering*, Vol. 53, pp 1127-1143, 2002.
- [2] G.P. Greyvenstein, J.P. van Ravenswaay and P.G. Rousseau, Dynamic modelling of heat, mass and momentum transfer in the Pebble Bed Modular Reactor, *1st International Conference on Heat Transfer, Fluid Mechanics, and Thermodynamics*, 8-10 April 2002, Kruger Park, South Africa.